Engineering 53 (2025) 90–103

Contents lists available at ScienceDirect

Engineering

journal homepage: www.elsevier.com/locate/eng

Research
Carbon Neutrality Pathways for Building Operation—Article

Decarbonization of Building Operations with Adaptive Quantum Computing-Based Model Predictive Control

Akshay Ajagekar [a], Fengqi You [a,b,*]

[a] Systems Engineering, Cornell University, Ithaca, NY 14853, USA
[b] Robert Frederick Smith School of Chemical and Biomolecular Engineering, Cornell University, Ithaca, NY 14853, USA

ARTICLE INFO

Article history:
Received 30 June 2024
Revised 10 December 2024
Accepted 11 February 2025
Available online 13 February 2025

Keywords:
Quantum computing
Carbon neutrality
Building energy control
Quantum approximate optimization

ABSTRACT

This work proposes an adaptive quantum approximate optimization-based model predictive control (MPC) strategy for energy management in buildings equipped with battery energy storage and renewable energy generation systems. The learning-based parameter transfer scheme to realize adaptive quantum optimization leverages Bayesian optimization to predict initial quantum circuit parameters. When applied to the MPC problems formulated as quadratic unconstrained binary optimization problems, this approach computes optimal controls to minimize the net energy consumption levels in buildings and promotes decarbonization while reducing the computational efforts required for the quantum approximate optimization algorithm as the building energy system trajectory progresses. The energy efficiency and the decarbonization benefits of the proposed quantum optimization-based MPC strategy are demonstrated on buildings at the Cornell University campus. The proposed quantum computing-based technique to address MPC problems in buildings demonstrates energy-efficient and low-carbon building operation with a 6.8% improvement over deterministic MPC and presents opportunities for scaling to larger control problems with a significant reduction in utilized quantum computing resources. A reduction of 41.2% in carbon emissions is also achieved with the proposed control strategy facilitated by efficiently managing battery energy storage and renewable generation sources to promote a push toward carbon-neutral building operations.

© 2025 THE AUTHORS. Published by Elsevier LTD on behalf of Chinese Academy of Engineering and Higher Education Press Limited Company. This is an open access article under the CC BY-NC-ND license (http://creativecommons.org/licenses/by-nc-nd/4.0/).

1. Introduction

Buildings are responsible for a significant portion of global energy use, primarily through heating, cooling, lighting, and the operation of appliances and systems [1]. Residential and commercial buildings consume approximately 30% of global energy annually, while emissions from the building sector also contribute to 21% of global greenhouse gas emissions [2]. Several directives have been implemented to mitigate these environmental impacts and promote a push towards carbon neutrality [3]. Initiatives like the Paris Agreement impact building regulations by setting national carbon emission reduction targets that can be translated into adopting building energy codes and minimum performance standards to enhance energy efficiency [4]. Promoting energy-efficient technologies and energy storage facilities accompanied by integrating renewable energy in the building sector to encourage on-site renewable energy generation is another key strategy to enable sustainable building operations [5–7]. Building energy management systems present a significant opportunity to realize carbon-neutral building operations by optimizing performance and cost-efficiency, effectively reducing the environmental impact [8,9]. Owing to advanced technologies like smart meters and smart sensors, energy management systems in buildings can manage renewable energy sources, energy storage devices, and building loads to facilitate energy-efficient operations [10]. Factors like varying sources of uncertainty, such as climate and weather conditions and unpredictable occupant behavior, can significantly influence energy consumption patterns in buildings [11]. Additionally, diverse appliance loads from electrical equipment and heating, ventilation, and cooling (HVAC) systems, along with variable hot water demand, add complexity to the energy management systems [12,13]. Developing high-performance and energy-efficient building operation strategies is crucial to addressing the complexities

* Corresponding author.
E-mail address: fengqi.you@cornell.edu (F. You).

https://doi.org/10.1016/j.eng.2025.02.002
2095-8099/© 2025 THE AUTHORS. Published by Elsevier LTD on behalf of Chinese Academy of Engineering and Higher Education Press Limited Company.
This is an open access article under the CC BY-NC-ND license (http://creativecommons.org/licenses/by-nc-nd/4.0/).

inherent to pushing building energy systems toward carbon neutrality [14].

Several strategies for energy management in buildings have been widely investigated and range from metaheuristics like evolutionary algorithms [15,16] to math programming-based optimization like model predictive control (MPC) [17,18]. MPC has emerged as a highly effective strategy for energy management in buildings as it systematically incorporates future predictions and operating constraints to optimize building operations aimed at objectives like optimal HVAC control [19], energy flexibility [20], and minimizing energy consumption [21], associated energy costs [22], as well as decarbonizing building operations [23]. The performance of the MPC strategy is dependent on the accuracy of the predictive model extracted through physics-based modeling, while challenges like system uncertainties can be tackled with stochastic optimization methods like stochastic programming [24], chance-constrained optimization [25], robust optimization [26], and even data-driven control [27]. Although MPC has been demonstrated to be a highly effective and versatile tool, it can face challenges in handling nonlinear systems and large-scale optimization problems [28]. The computational burden of MPC increases exponentially with the problem size, which can limit its applicability to real-time control of large-scale building energy systems [29]. Although metaheuristic approaches like evolutionary algorithms are capable of handling complex optimization problems, they struggle with convergence speed and solution quality for large-scale systems [30]. The practical implementation of stochastic optimization methods in energy management systems can be limited by the high computational complexity associated with an increase in the number of uncertain parameters. In the absence of a model derived from first principles, model-free techniques like reinforcement learning can be leveraged for optimal energy management in buildings [31,32]. Within a reinforcement learning setting, the energy management problem is cast as a sequential decision-making problem to compute decisions by observing the system states at any given time. Challenges like data inefficiency, safety concerns, and generalization capabilities hamper the practical adoption of reinforcement learning-based strategies for real-world applications [33]. Quantum computing offers a promising direction for addressing these knowledge gaps and overcoming the limitations of classical methods. Quantum algorithms have the potential to solve large-scale optimization problems exponentially faster than classical computers, making them particularly suitable for complex building energy management systems [34,35].

Quantum-enhanced techniques have received significant attention over the recent years across diverse sectors spanning energy [36,37] and environment to finance [38] and drug design [39–41]. Several quantum algorithms that provide computational speedups over their classical counterparts have been previously proposed in the literature [42]. However, their practical applicability is typically hampered by the limitations associated with noisy intermediate-scale quantum (NISQ) devices, which suffer from high error rates and limited scalability [43,44]. This is a crucial factor, especially for quantum optimization algorithms like quantum semi-definite programming and quantum interior point methods [45], and can hinder their adoption in handling real-world optimization problems. While quantum computing has the potential to transform building energy management systems and promote decarbonization owing to the advancements in quantum hardware and algorithms [46,47], it is important to consider the associated practical challenges to facilitate the development of quantum-enhanced strategies tailored for energy management. While current quantum devices may not yet outperform classical computers for specific optimization problems, developing quantum algorithms can pave the way for future advancements. As quantum hardware advances, quantum computing-based solution techniques can be readily applied to more complex and larger-scale building energy systems.

There are a few research challenges associated with developing a quantum computing-based solution strategy to address the MPC problem in building energy management systems for improving energy efficiency and enhancing decarbonization efforts. Quantum computers can address specific classes of optimization problems like quadratic unconstrained binary optimization (QUBO) problems and quadratic programming problems with continuous variables. The first research challenge lies in casting the MPC problem as an optimization problem that can be solved with quantum computing-based strategies. As the MPC problem structure remains consistent over a time horizon while the system uncertainties vary over time, it is important to exploit knowledge of problem structure to reduce computational efforts at subsequent steps [48]. Developing an optimization strategy enabled by learning from prior experiences to improve the performance of the quantum optimization algorithm is another research challenge. The final research challenge lies in handling the system uncertainties in an adaptive manner to mitigate the gap in control performance guided by discrepancies between model prediction and actual realizations. In this work, we propose an adaptive quantum computing-based MPC strategy to address these research challenges. A building energy system equipped with an HVAC system and provisions for electric load incurred by domestic hot water (DHW) and appliances is considered here. Battery energy storage systems and photovoltaic (PV) generation as renewable resource integration are also modeled to promote flexibility. The optimization problem constructed for the MPC strategy is further reformulated into a QUBO problem to solve with the quantum approximate optimization algorithm. We further introduce a learning-based parameter transfer scheme for the quantum approximate optimization algorithm to enhance computational efficiency by providing a good starting point for each problem instance. This approach not only reduces the need for repeated quantum computing subroutines but also implicitly handles uncertainties and adapts to varying system states and external disturbances. To substantiate the energy-efficient behavior of the proposed strategy and measure its impact on decarbonization, the adaptive quantum optimization-based control for building energy management is further evaluated with various computational experiments using real-world building data along with benchmarking computational performance against classical and quantum counterparts. The key contributions of this work are as ollows:

- A novel adaptive learning-based parameter transfer scheme for quantum optimization to enable energy-efficient and decarbonized building operations with model predictive control.
- A novel formulation for the building energy management problem that significantly reduces the number of binary variables, enhancing computational efficiency and scalability, and ensuring optimal controls that minimize net energy consumption in buildings.
- Computational experiments with real-world buildings on the Cornell University campus in the United States, using relevant operational data to validate the energy efficiency of the quantum computing-based MPC strategy and measure its impact on carbon emissions, along with analyzing the associated computational efforts compared to quantum and classical baselines.

The remainder of this paper is structured as follows. The adaptive learning-based quantum optimization approach for MPC in building energy management systems is described in Section 2. Modeling building operations for energy management, including formulation of the optimization problem for MPC and quantum-compatible formulations of the corresponding optimization problems, are also presented in Section 2. Section 3 includes a

discussion of the computational experiments that were conducted and the empirical results. Conclusions are drawn in Section 4.

2. Methods

In this work, we consider smart buildings that utilize a comprehensive suite of modern smart technologies to meet their load demand. An adaptive quantum computing-based model predictive control strategy is designed for energy management in such buildings to promote decarbonization.

The building's net load constitutes energy consumed by the HVAC system, DHW system, and appliances that pose a time-shiftable load demand. A battery energy storage system is also equipped in the building to promote grid stability and flexibility. Additionally, we consider a setup for integrating renewable energy integration with PV panels to further reflect the real-world challenges of a building energy management system. An overview of the components comprising the building energy management system is presented in Fig. 1. The smart building is considered to be electrified so that its overall load demand can be supplied by electricity. As shown in Fig. 2, the energy management system can receive information about the current state from the building and its equipped energy devices, as well as provide relevant control signals that help to lower carbon emission levels through an energy-efficient behavior. The MPC problem constructed for the building energy system to optimize net energy consumption can be tackled with quantum computing-based optimization strategies followed by reformulation into QUBO problems. The quantum approximate optimization algorithm (QAOA) is capable of solving combinatorial optimization problems and is suited for NISQ devices. Although QAOA has been widely explored for its potential applications in solving optimization problems on quantum computers, it exhibits scalability issues in a practical setting [49,50]. It is also unclear whether QAOA provides any computational advantages over classical metaheuristics and deterministic solvers. To address these challenges, we develop an adaptive quantum-enhanced optimization strategy that exploits the related optimization problems posed by the MPC problem formulation to reduce the computational cost associated with the classical optimization of the QAOA parameters.

2.1. Modeling building operations

We first consider the building's thermal dynamics to manage the thermal demand for space heating and cooling accurately. The thermal dynamics are influenced by several key environmental and operational factors, which include the ambient air temperature, amount of heat provided by the HVAC system, and solar irradiation, denoted by T_a, U_{hc}, and I_s, respectively. U_{hc} can be used as a control variable for the HVAC system. Positive and negative values of this control variable indicate the addition and removal of heat from the system, respectively. A lumped capacitance modeling approach is leveraged here, which simplifies the complex interactions of heat within the building into manageable calculations such

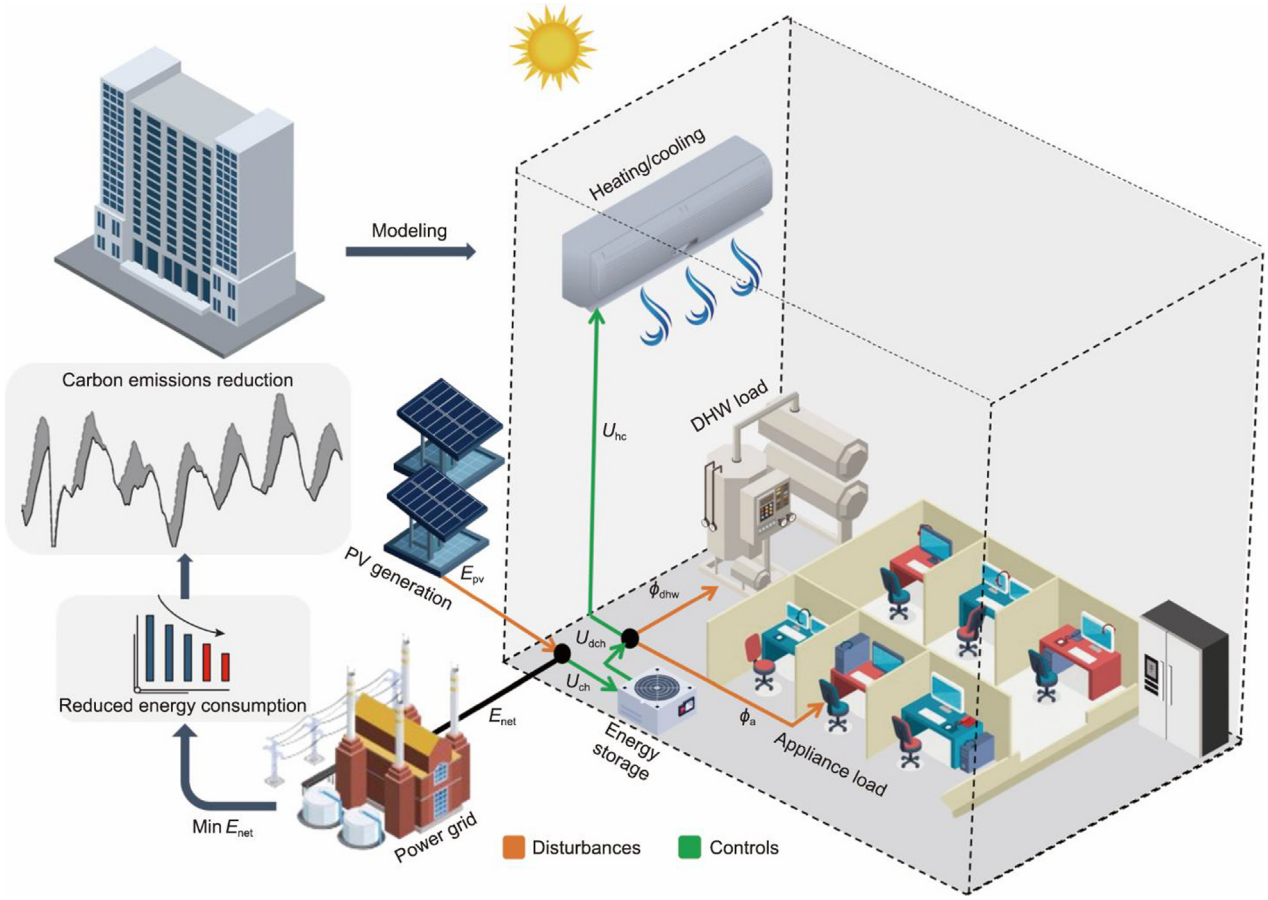

Fig. 1. Components of the modeled building energy management system comprising PV generation module, battery energy storage device, and the building loads. PV generation is denoted by E_{pv}, and E_{net} indicates the net energy consumption of the building energy system. U_{ch} and U_{dch} represent the charging and discharging levels for the battery energy storage system, while U_{hc} is the amount of heat added to the system. Load incurred by appliances and DHW demand is given by ϕ_a and ϕ_{dhw}, respectively.

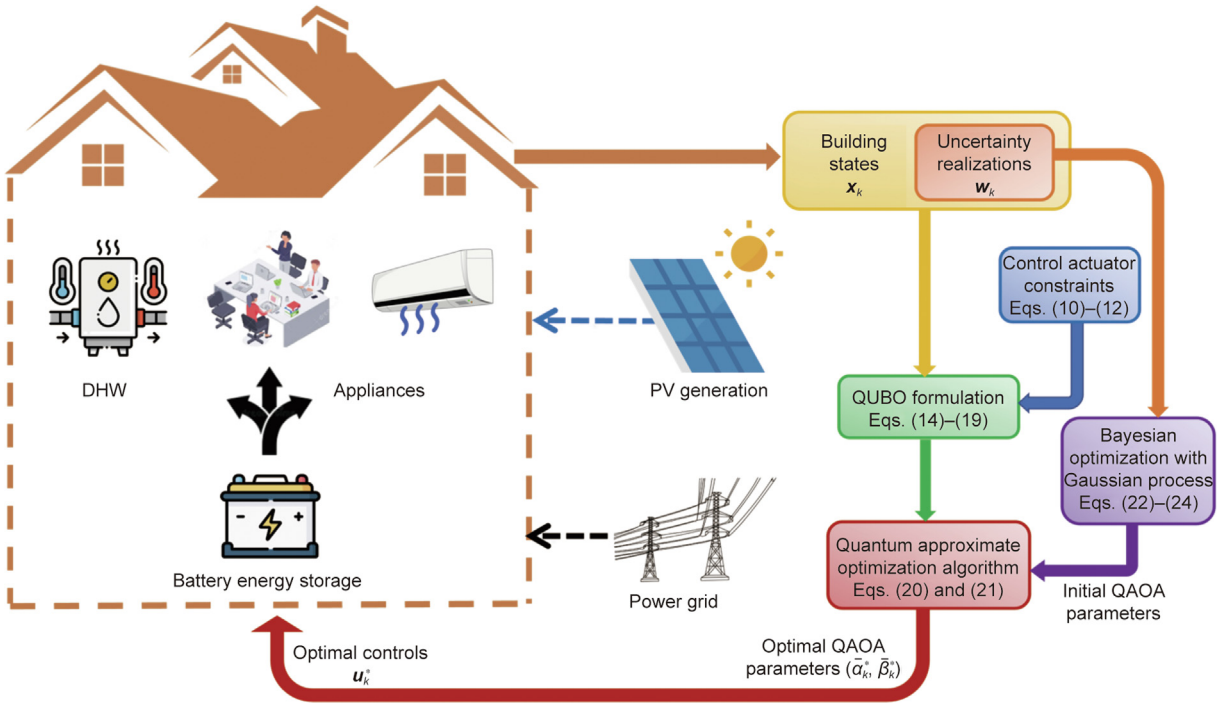

Fig. 2. An overview of the proposed quantum computing-based model predictive control strategy for energy management in buildings along with the components of the energy systems constituting the building. $\boldsymbol{x}_k$, $\boldsymbol{w}_k$, and $\mathbf{u}_k^*$ represent the vectors associated with building energy system states, disturbances, and control variables, respectively, at timestep k. The set of optimal gate parameters associated with the variational quantum circuit used in QAOA by solving the corresponding QUBO problem at timestep k are denoted by $\left(\vec{\alpha}_k^*, \vec{\beta}_k^*\right)$.

that the building can be treated as a few aggregated heat storage units or capacitances. For the building's thermal dynamics, we consider two primary states comprising the temperature of the internal heat-accumulating medium (T_m) apart from the indoor air temperature T_i. The internal heat-accumulating medium typically includes materials within the building that have substantial heat capacity, such as furniture, floors, and ceilings. By aggregating these components into a single medium, the model can effectively simulate how heat is stored and released over time, influencing the overall thermal environment inside the building. We then model the thermal dynamics of the building with the first-order differential equations in Eqs. (1) and (2). Eq. (1) describes the rate of change of indoor air temperature $\dot{T}_\mathrm{i}$, while Eq. (2) defines the rate of change in temperature of the heat-accumulating medium denoted by $\dot{T}_\mathrm{m}$. The parameters C_i and C_m denote the heat capacities of the indoor air and the medium, respectively. R_im denotes the thermal resistance between indoor air and the heat accumulating medium, while R_ia is the thermal resistance between the indoor air and the outdoor ambient air. η_h denotes the thermal efficiency of the supplementary heating and cooling system. A_b represents the windowed area of the building, while p_b is the solar transmittance of the windows.

$$\dot{T}_\mathrm{i} = -\left(\frac{1}{C_\mathrm{i}R_\mathrm{im}} + \frac{1}{C_\mathrm{i}R_\mathrm{ia}}\right)\cdot T_\mathrm{i} + \left(\frac{1}{C_\mathrm{i}R_\mathrm{im}}\right)\cdot T_\mathrm{m} + \eta_\mathrm{h}\cdot U_\mathrm{hc} + \left(\frac{1}{C_\mathrm{i}R_\mathrm{ia}}\right)\cdot T_\mathrm{a} + A_\mathrm{b}(1-p_\mathrm{b})\cdot I_\mathrm{s} \tag{1}$$

$$\dot{T}_\mathrm{m} = \left(\frac{1}{C_\mathrm{m}R_\mathrm{im}}\right)\cdot T_\mathrm{i} - \left(\frac{1}{C_\mathrm{m}R_\mathrm{im}}\right)\cdot T_\mathrm{m} + A_\mathrm{b}p_\mathrm{b}\cdot I_\mathrm{s} \tag{2}$$

We equip the building with a battery energy storage system and PV generation system. The battery storage system's dynamics is modeled with Eq. (3). The battery energy storage system is characterized by its capacity, nominal capacity, and the charging/discharging efficiency. The nominal capacity C_nom and efficiency of the battery η_bat as functions of the battery's state of charge (SOC) at time t (SOC_t) can be represented by piecewise linear functions. These curves allow for a more granular understanding of how battery performance metrics change with varying levels of charge. The charging and discharging energy levels at time t are represented by $U_{\mathrm{ch},t}$ and $U_{\mathrm{dch},t}$, respectively, and serve as controls for the energy storage system. Furthermore, the maximum power drawn for charging the battery and power discharged from the battery at any given time is constrained by the battery's current nominal capacity, which is depicted by the range $[0, C_\mathrm{nom}]$. This highlights the variable capacity of the battery to charge or provide energy, depending on its charge level. The energy generated by the PV panels can be used to directly supplement the building's load demand or to charge the equipped battery energy storage. At any time t, the PV generation $E_{\mathrm{pv},t}$ as a function of solar irradiation denoted by $I_{\mathrm{s},t}$ and can be modeled as shown in Eq. (4), where A_pv is the surface area of the PV panels that receive sunlight, η_pv is the efficiency coefficient, and the packing factor p_f refers to the density of solar cells within a PV module. We treat the load incurred by DHW demand and the appliances as uncertainties at time t, denoted by $\phi_{\mathrm{dhw},t}$ and $\phi_{\mathrm{a},t}$, respectively. Simulating the system trajectories involves utilizing historically realized data for the DHW and appliance load. Since we provision the additional or removal of heat from the system to control the internal temperature, the amount of energy incurred by the actuator is considered to be proportional to $|U_{\mathrm{hc},t}|$ defined as the amount of heat added to or removed from the system at time t. The net energy consumption of the modeled building energy system incurred at time t can then be modeled as $E_{\mathrm{net},t}$, which is drawn from the power grid as described in Eq. (5).

$$\mathrm{SOC}_{t+1} = \mathrm{SOC}_t + \sqrt{\eta_\mathrm{bat}}\cdot U_{\mathrm{ch},t} - \frac{1}{\sqrt{\eta_\mathrm{bat}}}\cdot U_{\mathrm{dch},t} \tag{3}$$

$$E_{\mathrm{pv},t} = A_\mathrm{pv}\eta_\mathrm{pv}p_\mathrm{f}\cdot I_{\mathrm{s},t} \tag{4}$$

$$E_{\mathrm{net},t} = |U_{\mathrm{hc},t}| + U_{\mathrm{ch},t} - U_{\mathrm{dch},t} + (\phi_{\mathrm{dhw},t} + \phi_{\mathrm{a},t}) - E_{\mathrm{pv},t} \tag{5}$$

We then extract a state-space formulation to represent the dynamics of the building energy system followed by the formulation of an optimization problem for the MPC control strategy, as shown in Eqs. (6)–(13). A discrete-time state-space model represented by Eq. (7) is obtained by discretizing the continuous differential equations in Eqs. (1) and (2), along with the battery dynamics in Eq. (3). As seen in Eq. (7), the state matrix $\boldsymbol{A}$, control matrix $\boldsymbol{B}$, and the disturbance matrix $\boldsymbol{C}$ constitute the state-space model. At any time t, the state variable vector denoted by $\boldsymbol{x}_t$ and given by $\boldsymbol{x}_t \equiv (T_{\mathrm{i},t}, T_{\mathrm{m},t}, \mathrm{SOC}_t)^{\mathrm{T}}$ comprises the temperatures associated with the building environment including indoor air temperature $T_{\mathrm{i},t}$, temperature of the heat accumulating medium $T_{\mathrm{m},t}$, and the battery storage state. The control variable vector denoted by $\boldsymbol{u}_t$ forms the control variables $\boldsymbol{u}_t \equiv (U_{\mathrm{hc},t}, U_{\mathrm{ch},t}, U_{\mathrm{dch},t})^{\mathrm{T}}$. $\boldsymbol{w}_t$ is defined as the disturbance vector and includes the weather uncertainties as well as the varying load demand associated with DHW and building appliances, and is given by $\boldsymbol{w}_t \equiv (T_{\mathrm{a},t}, I_{\mathrm{s},t}, \phi_{\mathrm{dhw},t}, \phi_{\mathrm{a},t})^{\mathrm{T}}$, where $T_{\mathrm{a},t}$ is the ambient air temperature at time t. Eq. (8) ensures that the thermal comfort of the occupants is maintained at all times, wherein $T_{\min,t}$ is the minimum acceptable temperature and $T_{\max,t}$ is the maximum acceptable temperature at time t. Charging of the battery energy storage system beyond its maximum capacity $C_{\max}$ is restricted in Eq. (9). Control actuator constraints are enforced by Eq. (10), wherein $\boldsymbol{u}_{\min}$ and $\boldsymbol{u}_{\max}$ are the vectors denoting minimum and maximum acceptable values for each control variable in $\boldsymbol{u}_t$, and include provisions for heating, cooling, charging, and discharging levels as dictated by the building HVAC system and nominal capacity of the energy storage. Furthermore, additional constraints are considered to prevent simultaneous charging and discharging at any given time, as shown in Eqs. (11) and (12). The binary variable y_t indicates whether the storage is being charged over the time horizon. The objective function in Eq. (6) for the constructed optimization problem reflects minimizing the building's net load demand. As the net energy drawn from the power grid can translate to carbon emissions, minimizing the building's net load can help to promote decarbonization efforts and can also be accompanied by economic benefits. Directly incorporating time-varying carbon intensity into the objective function would introduce additional uncertainties and computational complexities during the QUBO formulation step, as described in Section 2.2. The key idea for the MPC control strategy is to solve a new optimization problem formulated over a prediction horizon H at each timestep k where the set $H_k \equiv \{k, k+1, \ldots, k+H\}$ represents a set of discrete time intervals. At the timestep k, the optimal controls $\boldsymbol{u}_k$ are applied to the building energy system.

$$\min \sum_{t=k}^{k+H} E_{\mathrm{net},t} \tag{6}$$

$$\text{s.t.}\ \boldsymbol{x}_{t+1} = \boldsymbol{A}\boldsymbol{x}_t + \boldsymbol{B}\boldsymbol{u}_t + \boldsymbol{C}\boldsymbol{w}_t \tag{7}$$

$$T_{\min,t} \le T_{\mathrm{i},t} \le T_{\max,t}, \forall t \in H_k \tag{8}$$

$$\mathrm{SOC}_t \le C_{\max}, \quad \forall t \in H_k \tag{9}$$

$$\boldsymbol{u}_{\min} \le \boldsymbol{u}_t \le \boldsymbol{u}_{\max} \tag{10}$$

$$U_{\mathrm{ch},t} \le C_{\mathrm{nom}} \cdot y_t, \forall t \in H_k \tag{11}$$

$$U_{\mathrm{dch},t} \le C_{\mathrm{nom}} \cdot (1 - y_t), \forall t \in H_k \tag{12}$$

$$\boldsymbol{x}_t \ge 0, y_t \in \{0,1\}, \forall t \in H_k \tag{13}$$

2.2. Quadratic unconstrained binary optimization formulation

The optimization problem in Eqs. (6)–(13) is a mixed-integer linear programming problem that requires solving at every timestep and scales linearly with respect to a number of variables and constraints over the prediction horizon. Due to hardware constraints and native support offered by specific quantum optimization algorithms, we reformulate this optimization problem into a QUBO problem. This reformulation also facilitates the utilization of qubit interconnections specific to quantum hardware, enabling faster solutions compared to classical solution approaches in some cases. We consider a deterministic MPC problem to minimize the building's net energy consumption for reformulation into a tailored QUBO problem wherein future uncertain disturbances are treated as fixed value realizations over the optimization horizon. At time $t = k$, we have information about the system states $\boldsymbol{x}_k$ and the realized disturbances $\boldsymbol{w}_k$, while the future uncertainties are treated as fixed in the certainty equivalence formulation and denoted by $\zeta_k \equiv \{\boldsymbol{w}_t, \forall t = k+1, \ldots, k+H\}$. It is important to note that uncertainties are fixed only to simplify the QUBO formulation and are implicitly handled by the adaptive quantum optimization approach presented below.

During the QUBO reformulation step, key considerations to discretize the control variables $\boldsymbol{u}_t$ are required. The heating or cooling power $U_{\mathrm{hc},t}$ is subject to the building's HVAC actuator constraints and restricted to $[-H_{\max}, H_{\max}]$, where $H_{\max}$ is the maximum allowable power that can be drawn at any time t. To discretize the heating or cooling power $U_{\mathrm{hc},t}$, a binary variable z_{hc} is introduced. The binary variable z_{hc} indicates whether heating or cooling power is being supplied over the time horizon, while $z_{j,t}$ represents the jth bit in the bitstring representation. Combining this with a binary discretization scheme, the control variable can be reformulated with Eq. (14), where 2^n indicates the number of intervals into which the continuous domain $[0, H_{\max}]$ is divided with n number of bits. Similarly, we consider charging or discharging of the battery energy storage system by a fixed amount E_{bat} at each timestep to limit the binary variables in the QUBO problem. A binary variable $z_{\mathrm{b},t}$ is further introduced to indicate whether the battery energy storage system is charging or discharging at time t.

$$U_{\mathrm{hc},t} = \frac{H_{\max}}{2^n} \cdot (2z_{\mathrm{hc}} - 1) \sum_{j=0}^{n} 2^j \cdot z_{j,t} \tag{14}$$

$$\begin{aligned} U_{\mathrm{ch},t} &= E_{\mathrm{bat}} \cdot z_{\mathrm{b},t} \\ U_{\mathrm{dch},t} &= E_{\mathrm{bat}} \cdot (1 - z_{\mathrm{b},t}) \end{aligned} \tag{15}$$

The mixed-integer optimization problem can be cast as a QUBO problem represented by $Q(\boldsymbol{u}|\boldsymbol{x}_k, \boldsymbol{w}_k, \zeta_k)$ in Eq. (16), where $\boldsymbol{u}$ is the control variable vector that corresponds to $\boldsymbol{u}_t$. The QUBO problem at each timestep k comprises three components, as shown in Eq. (16). Within the QUBO problem at timestep k, λ_{h} and λ_{b} are the multipliers associated with the corresponding QUBO subproblems in Eq. (16). These multipliers are treated as fixed parameters and are commonly set as large values to ensure constraint satisfaction. These parameteras are chosen such that they follow the criteria, $\lambda \in \{\mathbb{R}^+ | \lambda \gg H_{\max}, \lambda \gg 2E_{\mathrm{bat}}\}$, where $\lambda \in \{\lambda_{\mathrm{h}}, \lambda_{\mathrm{b}}\}$ and $\mathbb{R}^+$ is the set of positive real numbers and can be fixed throughout all experiments for a given system. The QUBO subproblem Q_{o} associated with the objective function in Eq. (6) can be written with Eq. (17), and can be obtained by substituting $U_{\mathrm{hc},t}$, $U_{\mathrm{ch},t}$, and $U_{\mathrm{dch},t}$ with Eqs. (14) and (15), respectively. As the term $(2z_{\mathrm{hc}} - 1)$ dictates the positive or negative nature of the variable $U_{\mathrm{hc},t}$, value of $|U_{\mathrm{hc},t}|$ in Eq. (5) can be obtained by eliminating this multiplier as shown in Eq. (17).

$$\begin{aligned} Q(\boldsymbol{u}|\boldsymbol{x}_k, \boldsymbol{w}_k, \zeta_k) = Q_{\mathrm{o}}(\boldsymbol{u}|\boldsymbol{x}_k, \boldsymbol{w}_k, \zeta_k) + \lambda_{\mathrm{h}} \cdot Q_{\mathrm{h}}(\boldsymbol{u}|\boldsymbol{x}_k, \boldsymbol{w}_k, \zeta_k) \\ + \lambda_{\mathrm{b}} \cdot Q_{\mathrm{b}}(\boldsymbol{u}|\boldsymbol{x}_k, \boldsymbol{w}_k) \end{aligned} \tag{16}$$

$$\begin{aligned} Q_{\mathrm{o}}(\boldsymbol{u}|\boldsymbol{x}_k, \boldsymbol{w}_k, \zeta_k) = \sum_{t=k}^{k+H} \left[\frac{H_{\max}}{2^n} \left(\sum_{j=0}^{n} 2^j \cdot z_{j,t} \right) + E_{\mathrm{bat}} \cdot (2z_{\mathrm{b},t} - 1) \right] \\ + \sum_{t=k}^{k+H} (\phi_{\mathrm{dhw},t} + \phi_{\mathrm{a},t} - E_{\mathrm{pv},t}) \end{aligned} \tag{17}$$

$Q_{\mathrm{b}}(\boldsymbol{u}|\boldsymbol{x}_k, \boldsymbol{w}_k)$ is the QUBO subproblem that enforces battery charging and discharging dynamics while preventing charging beyond acceptable limits. This is given by $Q_{\mathrm{b}} = \sum_{\bar{k}}^{H} Q_{\mathrm{b},\bar{k}}(\boldsymbol{u}|\boldsymbol{x}_k, \boldsymbol{w}_k)$, where $Q_{\mathrm{b},\bar{k}}$ is described in Eq. (18) and corresponds to the maximum battery's SOC limit at the timestep $k+\bar{k}$ over the MPC horizon, where timestep $\bar{k}$ varies as $\bar{k} = 1, \ldots, H$. Here, $Q_{\mathrm{b},\bar{k}}$ represents the QUBO for the constraint $\mathrm{SOC}_{k+\bar{k}} \leq C_{\max}$, where $\mathrm{SOC}_{k+\bar{k}}$ is written as a function of the initial battery's SOC SOC_k and the control variables $\left\{U_{\mathrm{ch},k+\bar{k}}, U_{\mathrm{dch},k+\bar{k}}\right\}$ defined by $\left\{U_{\mathrm{ch},t}, U_{\mathrm{dch},k+\bar{k}}\right\}$ at timestep $k+\bar{k}$ substituted with their discrete reformulations in Eq. (15), while $F_{k,\bar{k}}$ is an auxiliary scalar coefficient used to simplify the expression for $Q_{\mathrm{b},\bar{k}}(\boldsymbol{u}|\boldsymbol{x}_k, \boldsymbol{w}_k)$. In Eq. (18), $z_{\mathrm{b},\hat{t}}$ represents the binary variable denoting charging or discharging of battery energy storage system at time $\hat{t}$ which satisfies $\hat{t} > t$. Similarly, $Q_{\mathrm{h}}(\boldsymbol{u}|\boldsymbol{x}_k, \boldsymbol{w}_k, \zeta_k)$ is the QUBO subproblem ensuring that thebuilding's indoor air temperature lies within the temperature range $[T_{\mathrm{sp}} - \delta, T_{\mathrm{sp}} + \delta]$ is achieved with the QUBO subproblem which is defined as $Q_{\mathrm{h}}(\boldsymbol{u}|\boldsymbol{x}_k, \boldsymbol{w}_k, \zeta_k) = \sum_{\bar{k}=1}^{H} Q_{\mathrm{h},\bar{k}}(\boldsymbol{u}|\boldsymbol{x}_k, \boldsymbol{w}_k)$, where T_{sp} is the temperature setpoint and δ is the allowable deviation from this setpoint. The subproblem $Q_{\mathrm{h},\bar{k}}$ represents the constraint $T_{\min,t} \leq T_{\mathrm{i},t} \leq T_{\max,t}$, wherein $T_{\mathrm{i},k+\bar{k}}$ which is $T_{\mathrm{i},t}$ at $t = k+\bar{k}$ can be written in terms of the initial indoor temperature $T_{\mathrm{i},k}$ and the heat-accumulating medium temperature $T_{\bar{k},k}$ along with the control inputs $U_{\mathrm{hc},t}$. This subproblem ensures the indoor climate conditions are maintained over the entire time horizon and is given in Eq. (19). Here, $\left[\boldsymbol{A}^{\bar{k}}\right]_{1:}$ notation is used to describe the first row of the matrix $\boldsymbol{A}^{\bar{k}}$ and $G_{k,\bar{k}}$ is an auxiliary scalar coefficient used to simplify this equation. This is followed by substituting expressions for $T_{i,k+\bar{k}}$ obtained after replacing state variables with the discretized control variable reformulation using $\boldsymbol{x}_{t+1} = \boldsymbol{A}\boldsymbol{x}_t + \boldsymbol{B}\boldsymbol{u}_t + \boldsymbol{C}\boldsymbol{w}_t$. The resulting inequality constraints for the state variables SOC_t and $T_{\mathrm{i},t}$ are dependent on the binary variables $z_{\mathrm{b},t}$ and $z_{j,t}$, and the model parameters for the MPC optimization problem. Inequality constraints with binary variables can be modeled as QUBO problems using [51].

$$Q_{\mathrm{b},\bar{k}}(\boldsymbol{u}|\boldsymbol{x}_k, \boldsymbol{w}_k) = \sum_{t=k}^{k+\bar{k}-1}\left(1 - F_{k,\bar{k}}\right)\cdot z_{\mathrm{b},t} + \sum_{t=k,\hat{t}>t}^{k+\bar{k}-1} 2 z_{\mathrm{b},t}\cdot z_{\mathrm{b},\hat{t}}$$
$$F_{k,\bar{k}} = \frac{\sqrt{\zeta}\cdot C_{\max} - \sqrt{\zeta}\cdot \mathrm{SOC}_k + \bar{k}\cdot E_{\mathrm{bat}}}{E_{\mathrm{bat}}\cdot(1+\zeta)} \tag{18}$$

$$Q_{\mathrm{h},\bar{k}}(\boldsymbol{u}|\boldsymbol{x}_k, \boldsymbol{w}_k, \zeta_k) = \left(T_{\mathrm{sp}} - G_{k,\bar{k}} - \frac{H_{\max}}{2^n}\sum_{t=k}^{k+\bar{k}-1}\left[\boldsymbol{A}^{\left(k+\bar{k}-1-t\right)}\boldsymbol{B}\right]_{1:}\sum_{j=0}^{n} 2^j\cdot z_{j,t}\right)^2$$
$$G_{k,\bar{k}} = \left[\boldsymbol{A}^{\bar{k}}\right]_{1:}\left(T_{\mathrm{i},k}, T_{\bar{k},k}\right)^{\mathrm{T}} + \sum_{t=k}^{k+\bar{k}-1}\left[\boldsymbol{A}^{\left(k+\bar{k}-1-t\right)}\boldsymbol{C}\right]_{1:}\boldsymbol{w}_t \tag{19}$$

Although it is straightforward to incorporate the decarbonization objective into the QUBO formulation step, the selection of these scaling parameters with varying binary coefficients in the QUBO associated with the decarbonization objective can lead to additional computational steps that can affect the controller performance and result in suboptimal solutions for the MPC optimization problem. It should be noted that the constructed QUBO problem comprises $\boldsymbol{O}(H\cdot n)$ binary variables, where $\boldsymbol{O}(\cdot)$ represents the big-O notation, n denotes the number of bits used to represent the continuous variable domain, and H is the MPC horizon. The performance of the quantum optimization solvers is directly correlated with the number of variables within the QUBO problem.

2.3. Quantum approximate optimization algorithm

The key component of the QAOA algorithm is the use of a variational quantum circuit (VQC) to parameterize the value of the QUBO problem. Within the quantum circuit model of computing, quantum algorithms are generally depicted as an ordered set of quantum circuits executed sequentially. These circuits encompass steps such as the preparation of the initial state, the application of unitary gates, and measurement operations to derive classical information that can be interpreted. These VQCs are commonly employed in many quantum machine learning algorithms because they maintain a high expressive power, even when implemented on NISQ devices. The variational circuit applies parametric gate operations to the initial quantum state, and the resultant quantum state is measured against an observable which is a matrix operator to estimate the target objective function.

The first step towards solving a QUBO problem with the QAOA algorithm is casting the QUBO problem as an Ising Hamiltonian denoted by Q, as shown in Eq. (20). For the MPC optimization problem reformulated as a QUBO problem, the linear coefficients h_x and quadratic coefficients J_{xy} for qubits x and y can be determined after casting {0, 1} binary variables as {−1, 1} variables denoted by $Z_x, Z_y \in \{-1, 1\}$ in Eq. (20). As shown in Fig. 3, the QAOA algorithm commences with the preparation of an initial state which is the superposition of all basis states denoted by $|\psi_0\rangle$ or $|+\rangle^N$. It operates on an N-qubit system, where N corresponds to the number of binary variables in the QUBO problem. The problem Hamiltonian H_{p} is designed to have its ground state encode the solution to the QUBO problem. Additionally, a mixer Hamiltonian H_{m} is defined to represent an X-rotation on each qubit. These Hamiltonians facilitate the construction of a VQC with parameters α and β denoted by the parametric gate operation $U(\alpha,\beta) = U(H_{\mathrm{m}},\alpha)\cdot U(H_{\mathrm{p}},\beta)$. The phase separation operator is designed to apply a phase to each computational basis state that is proportional to its cost by effectively embedding the problem's landscape into the quantum state's phases and is represented by $U(H_{\mathrm{p}},\beta) = \mathrm{e}^{-\mathrm{i}\beta H_{\mathrm{p}}}$, where i is the imaginary unit. The mixing operator given by $U(H_{\mathrm{m}},\alpha) = \mathrm{e}^{-\mathrm{i}\alpha H_{\mathrm{m}}}$ enhances the exploration of the solution space. The quantum state $|\psi\rangle$ emerges after applying the parameterized gate operations repeated L times as shown in Eq. (21). An expectation value $M = \langle\psi|H_{\mathrm{p}}|\psi\rangle$ is computed through measurements along the Z-basis. The objective of QAOA is to fine-tune the parameters $\bar{\alpha}$ and $\bar{\beta}$, defined as $\bar{\alpha} \equiv (\alpha_1, \alpha_2, \ldots, \alpha_L)$ and $\bar{\beta} \equiv (\beta_1, \beta_2, \ldots, \beta_L)$ to minimize M using a classical optimization algorithm such as gradient descent which is denoted by the blue arrow in Fig. 3. The parameter selection strategy for QAOA is crucial for its performance, as it can affect the computational effort required by QAOA to optimize the VQC parameters. After the optimal gate parameters are obtained, the constructed VQC is reapplied with these optimal parameters and the probabilities for each possible combination of the binary variables are measured. The bitstring with the highest probability represents an approximate solution that minimizes the QUBO problem.

$$Q = \sum\nolimits_x h_x Z_x + \sum\nolimits_{x,y>x} J_{xy} Z_x Z_y \tag{20}$$

$$|\psi\rangle = U(\alpha_L,\beta_L), \ldots, U(\alpha_2,\beta_2)\cdot U(\alpha_1,\beta_1)|\psi_0\rangle \tag{21}$$

2.4. Learning-based parameter transfer

QAOA for MPC problems within the building energy management system can be applied with random initialization of the gate parameters $\left(\bar{\alpha},\bar{\beta}\right)$ for each QUBO problem instance $Q(\boldsymbol{x}_k, \boldsymbol{w}_k, \zeta_k)$ at

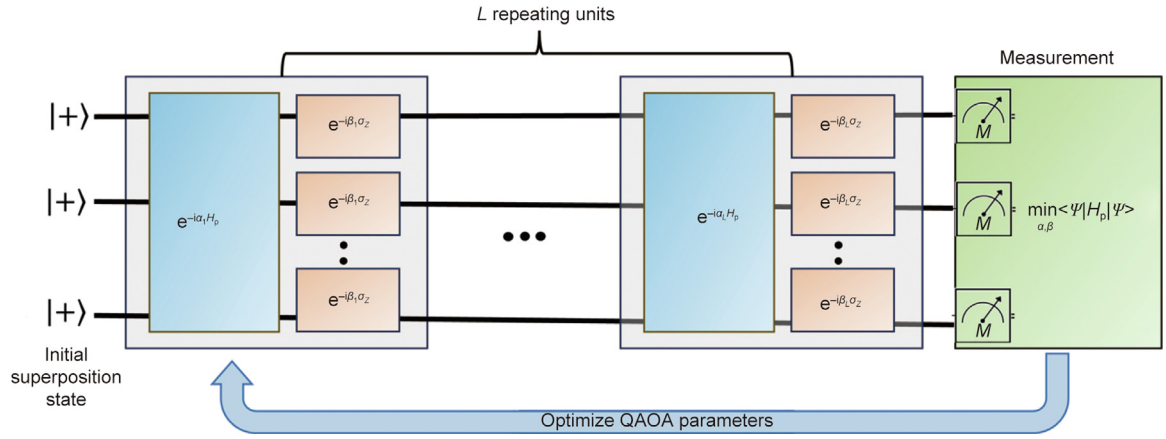

Fig. 3. Workflow for the quantum approximate optimization algorithm comprising the quantum circuit employed to iteratively minimize quadratic unconstrained binary optimization problems. $\alpha_1, \alpha_L, \beta_1,$ and β_L are the gate parameters and σ_z is the Pauli-Z operator.

timestep k. However, this can pose challenges in terms of computational resources required for solving individual problem instances over the system trajectory. To mitigate this, we employ a learning-based parameter transfer scheme for QAOA to efficiently optimize the gate parameters when solving a series of related optimization problem instances. The key idea behind a parameter transfer scheme for QAOA is that the optimal parameters for one QUBO problem instance may provide a good starting point for another problem instance that shares structural similarities. In addition to improving the computational performance of QAOA applied to the optimization problem at each timestep, it is important to ensure that the controller performance is maintained by adapting to varying building states and weather disturbances while addressing future uncertainties. We leverage a learning-based parameter transfer scheme to predict QAOA parameters as well as implicitly handle future uncertainties as the building energy system states evolve.

The QAOA-based MPC strategy can be realized with the use of Gaussian process to serve as a surrogate for the control performance as a function of the system states, current weather conditions, and the optimal QAOA parameters. At each timestep k, the system states $\boldsymbol{x}_k$ and the disturbances $\boldsymbol{w}_k$ form partial inputs to the Gaussian process denoted by X_k. The optimal QAOA parameters denoted by $\left(\bar{\alpha}_k^*, \bar{\beta}_k^*\right)$ obtained by solving the corresponding QUBO problem $Q\left(\boldsymbol{u}|\boldsymbol{x}_k, \boldsymbol{w}_k, \bar{\zeta}_k\right)$, where $\bar{\zeta}_k$ is the mean value of ζ_k and further constitutes the inputs X_k, and can be represented by $X_k \equiv \left(\boldsymbol{x}_k, \boldsymbol{w}_k, \bar{\alpha}_k^*, \bar{\beta}_k^*\right)$. The targets for the Gaussian process Y_k are calculated with Eqs. (22) and (23). In Eq. (22) the first term measures the value of knowing future uncertainties before making the decisions, while QV_k represents the expected energy consumption incurred by solving a deterministic optimization problem with fixed uncertainty values computed as their expectations $\bar{\zeta}_k = E_{\zeta_k}$. $\boldsymbol{u}^*$ in Eq. (23) indicates the optimal control variable vector which minimizes the value $Q\left(\boldsymbol{u}|\boldsymbol{x}_k, \boldsymbol{w}_k, \bar{\zeta}_k\right)$. The Gaussian process can then be represented as $Y_k \mathrm{GP}(m(X_k), c(X_k, X_k'))$ specified by its mean function $m(X_k)$ and covariance function $c(X_k, X_k')$ between inputs X_k and X_k'.

$$Y_k = \left(E_{\zeta_k}[\min Q(\boldsymbol{u}|\boldsymbol{x}_k, \boldsymbol{w}_k, \zeta_k)] - QV_k\right)^2 \tag{22}$$

$$QV_k = E_{\zeta_k}[\min Q(\boldsymbol{u}^*|\boldsymbol{x}_k, \boldsymbol{w}_k, \zeta_k)]$$
$$\boldsymbol{u}^* = \mathrm{argmin}_{\boldsymbol{u}} Q\left(\boldsymbol{u}|\boldsymbol{x}_k, \boldsymbol{w}_k, \bar{\zeta}_k\right) \tag{23}$$

The controller can then be implemented using a Bayesian optimization setting to identify initial QAOA parameters for the corresponding QUBO problem at each timestep. This is realized primarily due to the expensive evaluation of the target Y_k which requires multiple evaluations of $\min Q(\boldsymbol{u}|\boldsymbol{x}_k, \boldsymbol{w}_k, \zeta_k)$ over sampled uncertainty realizations ζ_k. An initial set of observations are collected to fit a Gaussian process prior. It should be noted that collecting this initial set requires solving QUBO problem instances at timesteps $k = 1, \ldots, T$ with initial QAOA parameters sampled randomly. Furthermore, computing $\min Q(\boldsymbol{u}|\boldsymbol{x}_k, \boldsymbol{w}_k, \zeta_k)$ over multiple realizations of ζ_k can be performed with a classical solver to limit the use of quantum computing resources. Following the learning stage, the QAOA parameters can be determined by minimizing the upper confidence bound (UCB) given by Eq. (24) as the acquisition function wherein μ and σ are functions of input X_t. Optimizing the confidence bound $\mathrm{UCB}(X_t)$ for input X_t can be conducted with gradient descent, however, it is important to note that the $(\boldsymbol{x}_t, \boldsymbol{w}_t) \in X_t$ remain fixed while the gate parameters at time t defined by $\left(\bar{\alpha}_t, \bar{\beta}_t\right)$ are optimized. For a given observation vector $(\boldsymbol{x}_t, \boldsymbol{w}_t) \in X_t$, the gate parameters obtained by minimizing $\mathrm{UCB}(X_t)$ serve as initial parameters for the QAOA algorithm. We control the exploration of the solutions $\left(\bar{\alpha}_t, \bar{\beta}_t\right)$ by using a small κ value for the confidence bound which ensures smaller values for the mean function. Using the predicted gate parameters, the last step within the QAOA algorithm comprising application of constructed VQC to represent the QUBO problem $Q\left(\boldsymbol{u}|\boldsymbol{x}_k, \boldsymbol{w}_k, \bar{\zeta}_k\right)$ is executed to obtain a binary bitstring solution. The binary variable values are then reutilized to compute the optimal controls for building energy management. In a typical Bayesian optimization setting, the posterior is updated with newly sampled datapoints, which would require computing targets Y_t. The computational resource utilization can be further limited by updating the posterior for the Gaussian process at fixed intervals while deploying the proposed controller for building energy management to improve energy consumption and carbon emission levels.

$$\mathrm{UCB}(X_t) = \mu(X_t) + \kappa \cdot \sigma(X_t) \tag{24}$$

3. Results and discussion

We conduct several computational experiments to demonstrate the energy efficiency and decarbonization benefits of the proposed adaptive quantum computing-based MPC strategy for building energy management. The experimental setup consists of two

buildings with varying system parameters. For the uncertainties associated with each building's load demand, historical data collected for Carpenter Hall and Baker Laboratory situated at Cornell University's Ithaca Campus, New York, USA, is utilized [52]. The simulation for building energy management case studies utilizes heat capacity of indoor air $C_i = 1.183\ \text{kW} \cdot \text{h} \cdot {}^\circ\text{C}^{-1}$ and heat capacity of the heat accumulating medium as $C_m = 4.005\ \text{kW} \cdot \text{h} \cdot {}^\circ\text{C}^{-1}$.Thermal resistances between the indoor air and the heat-accumulating medium $R_{im} = 0.4789\ \text{C} \cdot \text{kW}^{-1}$, and between indoor and outdoor air $R_{ia} = 29.25\ \text{C} \cdot \text{kW}^{-1}$ are considered. The first building's windowed area is 2.866 m^2 with a solar transmittance of 0.101, while the other building's windowed area is 3.213 m^2. The simulated energy management system also includes battery energy storage systems with maximum capacities of 0.9 and 1.1 MW·h, along with solar panels with an area of 1.4 and 0.8 m^2 for Carpenter Hall and Baker Laboratory, respectively. Weather data comprising ambient air temperature and solar radiation levels recorded in Ithaca also serve as the uncertainties present in the optimization problem posed by the MPC strategy for building energy management. Historical data recorded in the year 2021 is used to compute expectation values during the initial exploration phase of the learning-based approach to predict QAOA parameters. On the other hand, historical data from 2022 is utilized to conduct empirical evaluations of the proposed control strategy. The system parameters for the battery energy storage device and PV generation module for each building are chosen so that the energy devices can supplement a significant portion of the building's load demand. During the initial computational experiments, we consider an optimization problem over a horizon $H = 5$ with two bits to discretize the heating or cooling power control variable. The time interval for the discrete state-space model derived for the MPC strategy is set to one hour. Simulations over four months of January, April, July, and October are conducted to analyze the energy efficiency of the proposed adaptive QAOA-based MPC strategy, measure its impact on corresponding carbon emissions, and study the adaptability of the designed controller.

Several key assumptions are made to simplify the building energy management system modeling and the experimental setup. The model assumes that PV-generated power is instantly available for either direct building consumption or battery storage, with no transmission losses or delays. The thermal modeling assumes uniform temperature distribution within spaces and constant thermal properties for resistances and capacitances. Additionally, the control system is assumed to have perfect communication between components with no delays or sensor errors. Apart from the proposed control strategy, we conduct benchmarking of the controller performance against a baseline of deterministic MPC and quantum annealing. The deterministic MPC leverages a certainty equivalence formulation (CEMPC) wherein expectation values for the uncertainties are considered to solve the optimization problem over a fixed time horizon. As both the QAOA algorithm and quantum annealing address the QUBO problem, we do not compare their controller performance. Quantum annealing for addressing QUBO reformulations of the optimization problems within MPC requires resolving them at each timestep. Hence, we benchmark the solution times associated with quantum annealing against the adaptive computational efforts required with the learning-enhanced QAOA algorithm. Apart from the CEMPC and quantum annealing, we also compute the net energy consumption achieved with perfect knowledge about the future uncertainties to establish lower bounds on the incurred energy consumption with each control strategy. During the simulations, individual heating and cooling power required by the building HVAC control system to maintain indoor temperature are also recorded.

The learning-based QAOA technique is executed with noisy simulations for the IBM Brisbane quantum device equipped with the Eagle processor comprising 127 qubits [53]. The D-wave advantage system is utilized to conduct benchmarking with quantum annealing [54]. The experiments involving classical components are conducted with a Dell optiplex system with Intel Core i7-6700 3.40 GHz central processing unit (CPU) and 32 GB random access memory (RAM). These components involve the CEMPC implementation as well as the parameter update step and Gaussian process-based Bayesian optimization associated with the proposed quantum computing-based MPC strategy.

3.1. Energy efficiency and adaptability yields decarbonization in building operations

For each building energy system, we conduct simulations with the various controllers, including the proposed quantum computing-based adaptive MPC strategy over different time periods. Each building's net load demand and the energy consumption facilitated by the quantum computing-based adaptive optimization for building energy management in the first week of January are plotted in Fig. 4. As seen from the net load curves, the load demand exhibits significant variability and peaks at different times. This aligns with the typical behavior expected in building energy management, where usage can fluctuate based on various factors like occupancy, appliance use, DHW load, and the HVAC system. The net consumption tends to follow the load demand patterns but with notable deviation indicating the impact of factors such as energy storage and PV generation. This alignment of net consumption with load demand but with mitigated peaks suggests the effective learning and adaptability of the proposed quantum computing-based MPC strategy for building energy management. The presence of higher net consumption over load demands can be attributed to the initial phase of the quantum-enhanced MPC strategy in a Bayesian optimization setting. During these time periods, the controller solves certainty equivalent formulations of the MPC problem to collect initial samples to fit the Gaussian process prior. However, the following time periods where net consumption dips below load demand indicate periods of energy-efficient behavior using stored energy and reduced load with optimal controls achieved with the adaptive strategy.

The monthly net consumption incurred by the control strategies for each building is provided in Table 1, along with the lower bounds established by perfect knowledge of future uncertainties. The carbon emissions from the power grid associated with the building's energy consumption are also calculated in Table 1. Apart from the energy consumption and carbon emission levels, we also measure the percentage of constraint violations incurred by both CEMPC and the quantum computing-based control strategy. Net consumption is generally highest under the CEMPC approach due to its deterministic approach using fixed expectation values for uncertainties. The adaptive QAOA-based control strategy exhibits energy consumption closely matching the lower bounds set by perfect information. This is evident in both buildings and reflects the capability of the proposed control strategy to optimize with varying system states and uncertainties adaptively. A similar trend follows for the net carbon emission levels incurred with the corresponding control strategies. In the months of January and October, the adaptive QAOA-based MPC strategy incurs significantly lower carbon emissions and energy consumption than CEMPC, highlighting its superior energy efficiency and decarbonization capabilities. Furthermore, the proposed quantum computing-based MPC strategy also displays a consistent pattern of lower constraint violations than CEMPC. This can be directly attributed to the uncertainty handling capabilities of the QAOA-based optimization. Even with the uncertainty handling

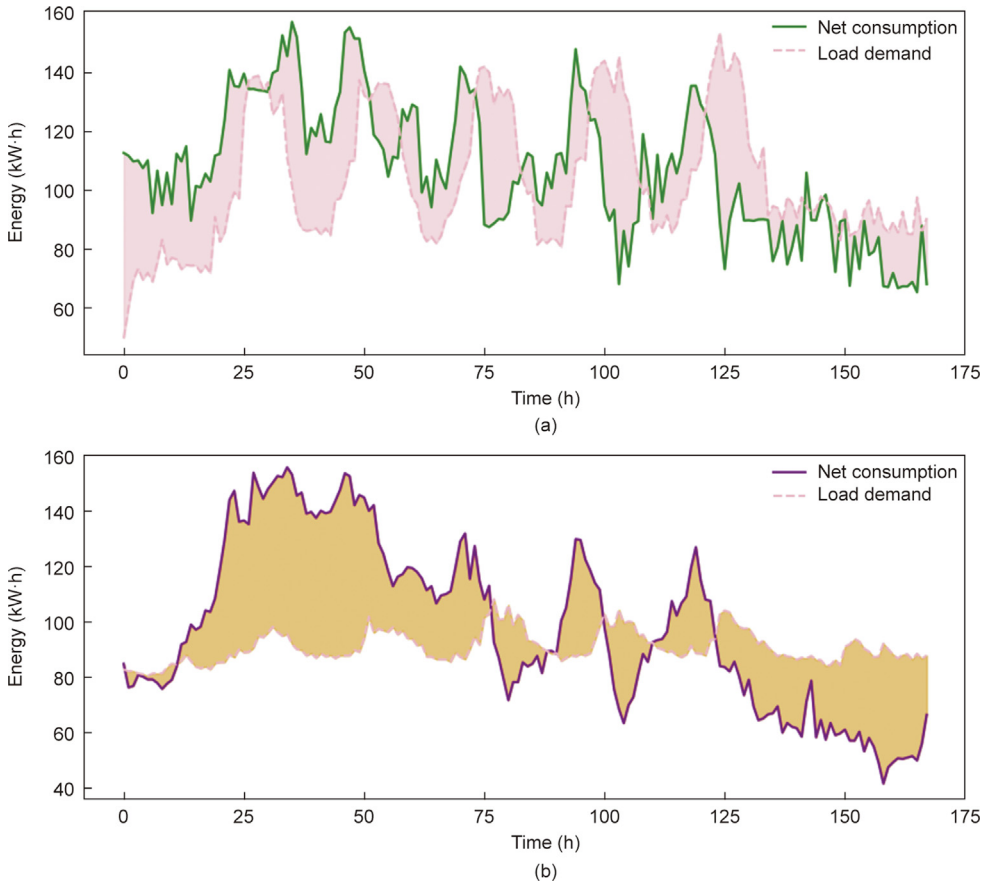

Fig. 4. Load demand and net energy consumption incurred in (a) the first building and (b) second building over a period of one week in January with the adaptive quantum computing-based MPC strategy for energy management.

Table 1
Monthly net energy consumption and associated carbon emissions incurred with different control strategies for both buildings, along with the percentage constraint violation measured during the corresponding simulations. CEMPC refers to the deterministic MPC strategy, while QC-MPC is the adaptive quantum computing-based MPC strategy.

Month	Building 1			Building 2		
	Perfect information	CEMPC	QC-MPC	Perfect information	CEMPC	QC-MPC
	Net energy consumption (kW·h)					
January	56 816	65 598	64 017	55 274	59 316	58 781
April	57 818	60 781	60 848	52 052	56 813	57 102
July	71 511	75 230	74 197	65 495	67 983	66 746
October	68 593	71 041	70 479	61 295	63 491	63 205
	Net carbon emissions ($kgCO_2$)					
January	10 316	12 691	11 971	9 990	12 946	12 047
April	7 671	9 419	9 129	6 937	8 471	8 058
July	10 821	12 918	12 001	9 982	11 940	11 756
October	10 340	12 571	11 905	9 302	11 850	10 940
	Constraint violation					
January	0	5.23%	4.12%	0	6.13%	5.87%
April	0	4.18%	4.19%	0	5.09%	4.12%
July	0	6.31%	5.10%	0	4.12%	4.25%
October	0	7.41%	6.67%	0	6.06%	5.43%

capabilities, the adaptive QAOA-based MPC strategy exhibits violations ranging from 4.12% to 6.67% across different months, indicating challenges in completely adhering to indoor temperature constraints. With lower violations than deterministic MPC, the observed patterns underscore the potential of the proposed quantum computing-based MPC control strategy in managing system constraints even in the presence of various uncertainties. We also visualize the reduction in carbon emissions achieved with the learning-based quantum optimization approach for the first building over a period of one week in January. The trend followed by the amount of reduction is consistent with the initial exploration steps in the Bayesian optimization setting, followed by the exploitation that results in reduced energy consumption and, consequently, lower carbon emissions. In addition, the monthly carbon emission levels for different months presented in Fig. 5 also substantiate the ability of the proposed quantum computing-based MPC strategy for building energy management to advance decarbonization efforts through sustainable operations in buildings. An annual

41.2% reduction in carbon emission levels is also measured, which further highlights the significant impact of decarbonization and a strong push towards carbon neutrality in buildings. Fig. 5 also provides a control trajectory for the indoor building temperature obtained with the adaptive quantum computing-based control strategy along with the temperature setpoints to visualize the proportion of constraint violations as the building energy system states evolve.

To further analyze the adaptability of the proposed quantum computing-based control strategy, we plot the incurred heating and cooling loads for the first building over the winter and summer seasons, as shown in Fig. 6. The outdoor ambient air temperatures are also plotted to serve as a reference. During colder weather conditions in January, the heating load generally increases as the outdoor temperature decreases. This correlation is evident from the inverse relationship between the two lines when the temperature dips, often going below 0 °C, and the energy used for heating surges. A highly sensitive heating response is realized with the adaptive control strategy with changes in outdoor temperature, reflecting an efficient and dynamic control system that adjusts heating output to compensate for heat loss as temperatures drop to maintain a comfortable indoor environment. The cooling load in summer also shows a direct correlation with increasing outdoor temperature. The peaks in energy usage correspond closely with the future high temperatures, illustrating the HVAC system's reactive increase in cooling efforts to counteract the incoming heat. Fig. 6 indicates that the building's HVAC is actively management by the proposed adaptive QAOA-based MPC controller to respond to external temperature changes. This dynamic adjustment helps maintain indoor comfort regardless of extreme external temperatures and highlights the critical role of the proposed control approach in realizing a responsive building energy management system.

3.2. Computational efficiency realized by adaptive quantum optimization to promote building decarbonization

The proposed control strategy is an adaptive approach that predicts optimal QAOA parameters to solve corresponding QUBO problems at each timestep. Unlike CEMPC and quantum annealing, the computational efforts required by the learning-based QAOA reduce as the system trajectory evolves. To analyze this, we measure the number of iterations taken by the QAOA to reach its optimum after predicting with QAOA parameters by minimizing the upper confidence bound for the underlying Gaussian process. Similarly, we also measure the solution time required to solve QUBO problem instances with quantum annealing as applied to building energy systems in Ref. [46]. As quantum annealing and QAOA are supported by inherently different quantum hardware, a direct comparison cannot be made with respect to their computational performance. Fig. 7 depicts both the quantum annealing solution time and QAOA iterations over a period of one week. As evident from this figure, quantum annealing time exhibits consistent fluctuations throughout the period. This reflects the consistent effort required to solve the problem instances anew each time without the benefit of learning or adapting from previous solutions. Apart from tackling the MPC optimization problem by reformulation into QUBO problems

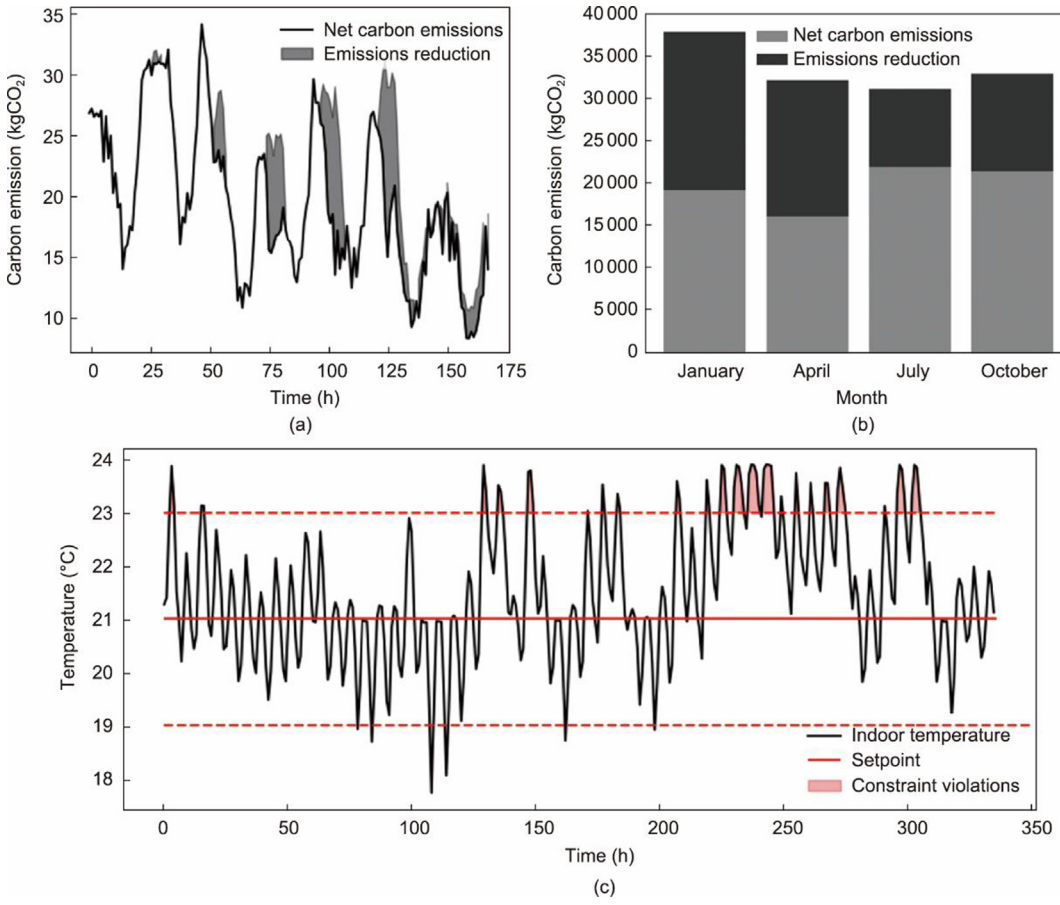

Fig. 5. (a) Reduction in carbon emission levels obtained with the quantum computing-based model predictive control strategy over a period of one week in January, as well as (b) monthly emissions. (c) A control trajectory for the building's indoor temperature over a period of one week in winter obtained with the same control strategy is also visualized. The red dotted line represents the minimum and maximum acceptable limits for the indoor temperature.

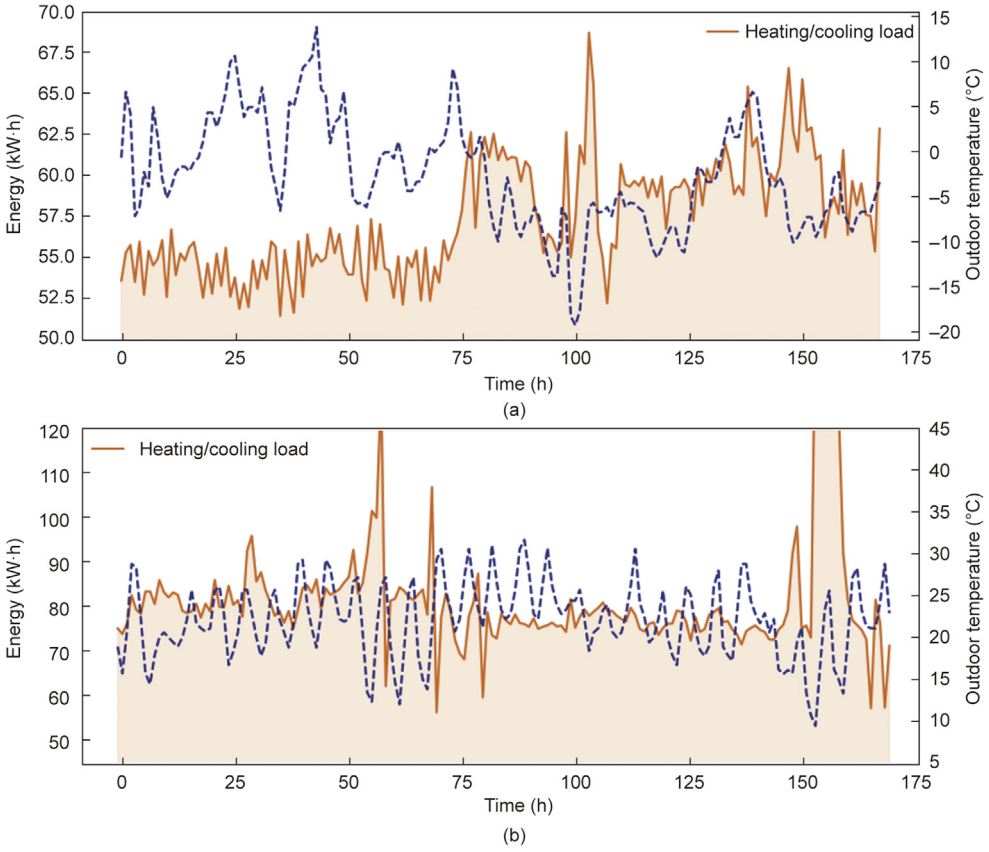

Fig. 6. The heating and cooling load in the (a) winter and (b) summer months as a response to the ambient air temperature with the incurred by the quantum computing-based model predictive control strategy for energy management. The blue dotted line represents the outdoor temperature.

and treatment with quantum optimization methods, the MPC optimization problem can also be addressed with quantum algorithms like Harrow–Hassidim–Lloyd (HHL) algorithm [55]. Although HHL offers an exponential speedup over classical algorithms in solving a linear system of equations [56], these quantum advantages cannot be realized with NISQ devices as their implementation requires fault-tolerant quantum devices with error-corrected qubits [44]. In contrast to the proposed adaptive QAOA method, HHL-based algorithms commonly used to solve small-scale optimization problems cannot be directly leveraged to solve the MPC optimization problem relevant to building energy systems. On the other hand, adaptive QAOA-based MPC strategy requires a significant number of iterations during the initial exploration phase. However, this number drastically reduces after this phase. This suggests that the adaptive mechanism in the learning-based QAOA approach quickly finds efficient parameters that allow for fewer iterations as time progresses. This rapid optimization and stability imply a high efficiency in adapting to the problem's dynamics without needing extensive computation beyond the initial phase.

As stated in Section 2.3, variables of the QUBO problem representing the optimization problem at each timestep scales as $O(H \cdot n)$. A solution to the QUBO problem solved with QAOA strongly depends on the number of variational layer repetitions. We conduct an ablation analysis between the varying number of variables representing the same optimization problem and the number of layer repetitions for QAOA using constraint violation percentage as a performance metric. The constraint violation levels under varying conditions are also plotted in Fig. 7. As shown in this figure, the constraint violation levels tend to increase as the number of variables increases, even though this trend is not uniform. It can be clearly seen that for a fixed problem size, the number of layer repetitions induces variability in the constraint violations. The notable inconsistencies across the metrics observed with varying numbers of layers indicate that other factors, like the QUBO problem parameters, can significantly influence performance despite the increased number of layer repetitions within the QAOA algorithm.

3.3. Considerations of model complexity and quantum optimization challenges

While the building energy system model presented in this study does not consider sophisticated MPC formulations, it serves as a representative example of common MPC problems in building energy management. The proposed quantum computing-based optimization method is designed to be extensible to more complex system configurations. In sophisticated MPC formulations considering HVAC with weather-dependent system performance, the increased complexity would primarily affect the matrices $\boldsymbol{A}$, $\boldsymbol{B}$, and $\boldsymbol{C}$. This would influence the parameters in the constructed QUBO problem. However, the fundamental method for QUBO construction would remain the same. The use of quantum computing in this context is justified by its potential for improved scalability, enhanced handling of uncertainty, and the development of future-proof algorithms that can leverage advancements in quantum hardware. Furthermore, the proposed hybrid quantum-classical approach demonstrates how quantum computing can complement existing classical methods, potentially leading to novel solutions for increasingly complex building energy systems. It is important to note that computing the targets for Gaussian process fitting requires considering various scenarios of future uncertainty

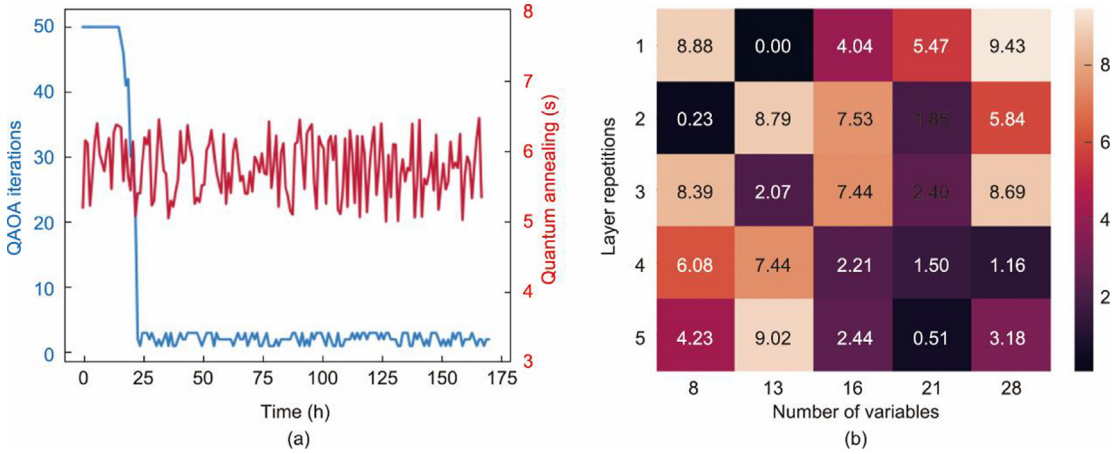

Fig. 7. (a) Computational efforts required by the learning-enhanced QAOA compared against quantum annealing. (b) The constraint violation levels measured for QUBO problems of varying sizes and varying layer repetitions settings within the QAOAO algorithm.

realizations. This approach allows our model to capture a range of possible outcomes to enhance its robustness in different future scenarios. By incorporating multiple realizations, we can better account for the stochastic nature of factors like weather patterns leading to more reliable predictions and control decisions. While our learning-based QAOA approach implicitly handles these uncertainties, limitations in predictive capabilities may arise in the case of longer horizons. Even though the proposed approach allows the system to adapt to changing conditions without relying solely on potentially inaccurate long-term predictions, incorporating uncertainty quantification methods could provide valuable insights into the reliability of the system's decisions under various scenarios.

Although this work demonstrates the effectiveness of QAOA for building energy management leveraging a learning-based parameter transfer scheme, it is important to discuss the applicability and limitations associated with the QAOA algorithm in comparison to other quantum optimization algorithms that may contribute to challenges in adopting the hybrid quantum-classical approach. QAOA offers several advantages like its ability to run on near-term quantum devices and its flexibility in handling various problem structures, but also faces challenges like difficulty of finding optimal parameters for deep circuits. Quantum annealing implemented on specialized hardware like D-wave systems can handle larger problem sizes but may struggle with certain problem structures that QAOA can address more effectively. The integration of quantum annealing with a learning-based approach can also be a hindrance to developing controllers for energy management that are capable of exploiting historical data. For building energy management specifically, QAOA's ability to handle time-dependent constraints and its adaptability through our proposed learning-based parameter transfer scheme makes it particularly suitable. However, for larger buildings with more complex energy systems, the increased number of variables might challenge QAOA's current capabilities. The tradeoff between these algorithms can evolve as quantum hardware continues to improve. Development of quantum ansatz that are tailored to the underlying energy system can further enhance the performance of the adaptive QAOA approach while mitigating its limitations.

4. Conclusions

In this work, we presented an adaptive quantum computing-based MPC strategy for building energy management to improve energy efficiency and promote decarbonization in buildings. The proposed strategy utilized a learning-based parameter transfer scheme for the QAOA algorithm that enables the optimizer to learn from previous computations, significantly reducing the need for repeated recalibrations and intensive computations required to solve optimization problems. The parameter transfer scheme for quantum optimization leveraged a Gaussian process in a Bayesian optimization setting to further enhance the efficiency and scalability of QAOA for MPC in building energy management systems. Various computational experiments illustrated a 6.8% improvement in energy efficiency over deterministic MPC approaches and also demonstrated computational efficiency over quantum annealing-based approaches as the building energy system evolved. Furthermore, the proposed strategy yielded an annual carbon emissions reduction of 41.2% by optimally managing building energy systems equipped with HVAC, battery storage, and PV generation. The quantum computing-based MPC strategy demonstrated significant improvements in energy efficiency and decarbonization while adapting to changing environmental conditions and system states while leveraging renewable energy sources effectively.

The integration of quantum algorithms with learning-based strategies remains essential to develop robust and adaptable control techniques for realizing the full potential of quantum computing for practical applications like building energy management. By leveraging learning-based quantum algorithms, this approach can significantly speed up the solution of large-scale optimization problems inherent in MPC, where real-time control computation is crucial. As demonstrated by the decrease in computational efforts required by quantum optimization techniques, the quantum computing-based MPC strategy has the potential to improve the control computation speed in response to dynamic environmental and system changes in domains of power systems, industrial process control, and energy systems at various scales. While this work demonstrates promising results for quantum-enabled MPC in building energy management, several key directions warrant further investigation. First, the integration of real-time carbon intensity metrics and dynamic pricing signals into the adaptive quantum optimization framework presents an important avenue for enhancing the environmental and economic impact of the control strategy. Second, comprehensive validation studies across diverse buildings including commercial complexes, industrial facilities, and residential communities would provide valuable insights into the scalability and generalizability of the proposed approach. Third, extending this methodology to more complex control scenarios like demand response mechanisms in smart grid applications could reveal additional use cases and potential limitations. Finally, architecture-specific optimization of the underlying

quantum algorithms through advanced error mitigation techniques could accelerate the practical adoption of this approach in real-world building energy management systems. These research directions collectively aim to bridge the gap between theoretical quantum-enabled control strategies and their practical implementation in sustainable building operations.

CRediT authorship contribution statement

Akshay Ajagekar: Writing – review & editing, Writing – original draft, Visualization, Validation, Software, Methodology, Investigation, Formal analysis, Data curation. **Fengqi You:** Writing – review & editing, Visualization, Supervision, Software, Resources, Project administration, Methodology, Investigation, Funding acquisition, Formal analysis, Conceptualization.

Declaration of competing interest

The authors declare that they have no known competing financial interests or personal relationships that could have appeared to influence the work reported in this paper.

References

[1] Luo Z, Peng J, Gao J, Yin R, Zou B, Tan Y, et al. Demand flexibility of residential buildings: definitions, flexible loads, and quantification methods. Engineering 2022;13(9):123–40.
[2] International Energy Agency. The critical role of buildings: perspectives of the clean energy transition. Report. Paris: International Energy Agency; 2019.
[3] Huang Z, Zhou H, Miao Z, Tang H, Lin B, Zhuang W. Life-cycle carbon emissions (LCCE) of buildings: implications, calculations, and reductions. Engineering 2024;35:115–39.
[4] Moghaddasi H, Culp C, Vanegas J, Ehsani M. Net zero energy buildings: variations, clarifications, and requirements in response to the Paris Agreement. Energies 2021;14(13):3760.
[5] Li DH, Yang L, Lam JC. Zero energy buildings and sustainable development implications—a review. Energy 2013;54:1–10.
[6] Wu W, Skye HM. Residential net-zero energy buildings: review and perspective. Renew Sustain Energy Rev 2021;142:110859.
[7] Yang S, Gao HO, You F. Demand flexibility and cost-saving potentials via smart building energy management: opportunities in residential space heating across the US. Adv Appl Energy 2024;14:100171.
[8] Ma M, Zhou N, Feng W, Yan J. Challenges and opportunities in the global net-zero building sector. Cell Rep Sustain 2024;1(8):2427079.
[9] Zhang S, Ma M, Zhou N, Yan J, Feng W, Yan R, et al. Estimation of global building stocks by 2070: unlocking renovation potential. Nexus 2024;1(3):100019.
[10] Nagpal H, Avramidis II, Capitanescu F, Heiselberg P. Optimal energy management in smart sustainable buildings—a chance-constrained model predictive control approach. Energy Build 2021;248:111163.
[11] Amadeh A, Lee ZE, Zhang KM. Quantifying demand flexibility of building energy systems under uncertainty. Energy 2022;246:123291.
[12] Chen C, Wang J, Heo Y, Kishore S. MPC-based appliance scheduling for residential building energy management controller. IEEE Trans Smart Grid 2013;4(3):1401–10.
[13] Nguyen HT, Nguyen DT, Le LB. Energy management for households with solar assisted thermal load considering renewable energy and price uncertainty. IEEE Trans Smart Grid 2014;6(1):301–14.
[14] Yang S, Gao HO, You F. Integrated optimization in operations control and systems design for carbon emission reduction in building electrification with distributed energy resources. Adv Appl Energy 2023;12:100144.
[15] Fong KF, Hanby VI, Chow TT. System optimization for HVAC energy management using the robust evolutionary algorithm. Appl Therm Eng 2009;29(11–12):2327–34.
[16] Soares A, Gomes A, Antunes CH, Oliveira C. A customized evolutionary algorithm for multiobjective management of residential energy resources. IEEE Trans Industr Inform 2016;13(2):492–501.
[17] Mariano-Hernández D, Hernández-Callejo L, Zorita-Lamadrid A, Duque-Pérez O, Santos GF. A review of strategies for building energy management system: model predictive control, demand side management, optimization, and fault detect & diagnosis. J Build Eng 2021;33:101692.
[18] Chen WH, You F. Sustainable building climate control with renewable energy sources using nonlinear model predictive control. Renew Sustain Energy Rev 2022;168:112830.
[19] Yao Y, Shekhar DK. State of the art review on model predictive control (MPC) in heating ventilation and air-conditioning (HVAC) field. Build Environ 2021;200:107952.
[20] Finck C, Li R, Zeiler W. Economic model predictive control for demand flexibility of a residential building. Energy 2019;176:365–79.
[21] Yang S, Wan MP, Chen W, Ng BF, Dubey S. Model predictive control with adaptive machine-learning-based model for building energy efficiency and comfort optimization. Appl Energy 2020;271:115147.
[22] Ma J, Qin SJ, Li B, Salsbury T. Economic model predictive control for building energy systems. In: Proceedings of the ISGT 2011; 2011 Jan 17–19; Anaheim, CA, USA. New York City: IEEE; 2011. p. 1–6.
[23] Xiao T, You F. Building thermal modeling and model predictive control with physically consistent deep learning for decarbonization and energy optimization. Appl Energy 2023;342:121165.
[24] Ma Y, Matuško J, Borrelli F. Stochastic model predictive control for building HVAC systems: complexity and conservatism. IEEE Trans Control Syst Technol 2014;23(1):101–16.
[25] Wang X, Liu Y, Xu L, Liu J, Sun H. A chance-constrained stochastic model predictive control for building integrated with renewable resources. Electric Power Syst Res 2020;184:106348.
[26] Kuznetsova E, Li YF, Ruiz C, Zio E. An integrated framework of agent-based modelling and robust optimization for microgrid energy management. Appl Energy 2014;129:70–88.
[27] Sun L, You F. Machine learning and data-driven techniques for the control of smart power generation systems: an uncertainty handling perspective. Engineering 2021;7(9):1239–47.
[28] Lefebure N, Khosravi M, Hudoba de Badyn M, Bünning F, Lygeros J, Jones C, et al. Distributed model predictive control of buildings and energy hubs. Energy Build 2022;259:111806.
[29] Gomez-Romero J, Fernandez-Basso CJ, Cambronero MV, Molina-Solana M, Campana JR, Ruiz MD, et al. A probabilistic algorithm for predictive control with full-complexity models in non-residential buildings. IEEE Access 2019;7:38748–65.
[30] Ezugwu AE, Adeleke OJ, Akinyelu AA, Viriri S. A conceptual comparison of several metaheuristic algorithms on continuous optimisation problems. Neural Comput Appl 2020;32(10):6207–51.
[31] Yu L, Qin S, Zhang M, Shen C, Jiang T, Guan X. A review of deep reinforcement learning for smart building energy management. IEEE Internet Things J 2021;8(15):12046–63.
[32] Mason K, Grijalva S. A review of reinforcement learning for autonomous building energy management. Comput Electr Eng 2019;78:300–12.
[33] Kaelbling LP, Littman ML, Moore AW. Reinforcement learning: a survey. J Artif Intell Res 1996;4:237–85.
[34] Ajagekar A, You F. Quantum computing and quantum artificial intelligence for renewable and sustainable energy: a emerging prospect towards climate neutrality. Renew Sustain Energy Rev 2022;165:112493.
[35] Deng Z, Dong B. Discrete optimal control of building to grid integration based on quantum computing. In: Proceedings of Building Simulation 2023: 18th Conference of IBPSA; 2023 Sep 4–6; Shanghai, China. Singapore: International Building Performance Simulation Association; 2023. p. 2768–75.
[36] Ajagekar A, You F. Quantum computing for energy systems optimization: challenges and opportunities. Energy 2019;179:76–89.
[37] Paudel HP, Syamlal M, Crawford SE, Lee YL, Shugayev RA, Lu P, et al. Quantum computing and simulations for energy applications: review and perspective. ACS Eng Au 2022;2(3):151–96.
[38] Orús R, Mugel S, Lizaso E. Quantum computing for finance: overview and prospects. Rev Phys 2019;4:100028.
[39] Cao Y, Romero J, Aspuru-Guzik A. Potential of quantum computing for drug discovery. IBM J Res Dev 2018;62(6):1–20.
[40] Andersson MP, Jones MN, Mikkelsen KV, You F, Mansouri SS. Quantum computing for chemical and biomolecular product design. Curr Opin Chem Eng 2022;36:100754.
[41] Ajagekar A, You F. Molecular design with automated quantum computing-based deep learning and optimization. Npj Comput Mater 2023;9(1):143.
[42] Montanaro A. Quantum algorithms: an overview. Npj Quantum Inf 2016;2:15023.
[43] Cerezo M, Arrasmith A, Babbush R, Benjamin SC, Endo S, Fujii K, et al. Variational quantum algorithms. Nat Rev Phys 2021;3(9):625–44.
[44] Bharti K, Cervera-Lierta A, Kyaw TH, Haug T, Alperin-Lea S, Anand A, et al. Noisy intermediate-scale quantum algorithms. Rev Mod Phys 2022;94(1):015004.
[45] Kerenidis I, Prakash A. A quantum interior point method for LPs and SDPs. ACM Transact Quantum Comput 2020;1(1):1–32.
[46] Deng Z, Wang X, Dong B. Quantum computing for future real-time building HVAC controls. Appl Energy 2023;334:120621.
[47] Ajagekar A, You F. Variational quantum circuit based demand response in buildings leveraging a hybrid quantum-classical strategy. Appl Energy 2024;364:123244.
[48] Shaydulin R, Lotshaw PC, Larson J, Ostrowski J, Humble TS. Parameter transfer for quantum approximate optimization of weighted maxcut. ACM Transact Quantum Comput 2023;4(3):1–15.
[49] Zhou L, Wang ST, Choi S, Pichler H, Lukin MD. Quantum approximate optimization algorithm: performance, mechanism, and implementation on near-term devices. Phys Rev X 2020;10(2):021067.
[50] Basso J, Gamarnik D, Mei S, Zhou L. Performance and limitations of the QAOA at constant levels on large sparse hypergraphs and spin glass models. In: Proceedings of the 2022 IEEE 63rd Annual Symposium on Foundations of Computer Science (FOCS); 2022 Oct 31–Nov 3; Denver, CO, USA. New York City: IEEE; 2022. p. 335–43.
[51] Glover F, Kochenberger G, Du Y. A tutorial on formulating and using QUBO models. 2018. arXiv:1811.11538.

[52] Sustainable Campus. Building Energy Dashboard [Internet]. Ithaca: Campus Sustainability Office, Cornell University; [cited 2024 Nov 20]. Available from: https://sustainablecampus.cornell.edu/building-energy-dashboard.
[53] Chow J, Dial O, Gambetta J. IBM Quantum breaks the 100-qubit processor barrier [Internet]. Armonk: IBM Research Blog; 2021 Nov 16. [cited 2024 Nov 20]. Available from: https://www.ibm.com/quantum/blog/127-qubit-quantum-processor-eagle.
[54] Willsch D, Willsch M, Gonzalez Calaza CD, Jin F, De Raedt H, Svensson M, et al. Benchmarking advantage and D-wave 2000Q quantum annealers with exact cover problems. Quantum Inform Process 2022;21(4):141.
[55] Feng F, Zhou Y, Zhang P. Quantum power flow. IEEE Trans Power Syst 2021;36(4):3810–2.
[56] Harrow AW, Hassidim A, Lloyd S. Quantum algorithm for linear systems of equations. Phys Rev Lett 2009;103(15):150502.